NUMERICAL INVESTIGATION OF A CENTRIFUGAL COMPRESSOR WITH CIRCUMFERENTIAL GROOVES IN VANE DIFFUSER

X F CHEN[1], **G L QIN**[1], **Z J AI**[1, 2]

[1] School of Energy and Power Engineering, Xi'an Jiaotong University, Xi'an 710049, China
[2] School of Mechanical and Electronic Engineering, Sanming University, Sanming 365004, China

Email:glqin@mail.xjtu.edu.cn

Abstract. Enhancing stall and surge margin has a great importance for the development of turbo compressors. The application of casing treatment is an effective measure to expand the stall margin and stable operation range. Numerical investigations were conducted to predict the performance of a low flow rate centrifugal compressor with circumferential groove casing treatment in vane diffuser. Numerical cases with different radial location, radial width and axial depth of a circumferential single groove and different numbers of circumferential grooves were carried out to compare the results. The CFD analyses results show that the centrifugal compressor with circumferential grooves in diffuser can extend stable range by about 9% while the efficiency over the whole operating range decreases by 0.2 to 1.7%. The evaluation based on stall margin improvement showed the optimal position for the groove to be located was indicated to exist near the leading edge of the diffuser, and a combination of position, width, depth and numbers of circumferential grooves that will maximize both surge margin range and efficiency.

1. Introduction

The design of modern compressor is mainly focused on reducing stage numbers, which often leads to the problem of how to prevent flow instabilities such as surge and rotating stall. Additional to the ingenuity exercised in aerodynamic blade designing, various devices and methods have been tried out. Among them, casing treatment, small grooves or slots made on the endwall, has been proved to have a beneficial effect on increasing stable operating range of compressors.

Numerous configurations have been tested and studied since its development [1], and among them, large proportion of the recent research objectives seem to be devoted exclusively to two principal categories. One is the casing treatment which consists of circumferentially aligned axial slots [2, 3], and the other is the casing treatment with axially aligned circumferential grooves [4, 5]. Both have shown a sufficient capability in improving stall margin, but circumferential grooves seem to have an advantage in practical use from a perspective of efficiency drop which associates with the stabilizing effect and the cost-effectiveness in mechanical processing.

Recently, the mechanism through which circumferential casing groove enlarges the stable operating range in transonic compressor is becoming apparent through numerical and experimental investigations [5–7]. The interaction of passage shock and tip leakage vortex has often been pointed out as an important factor of stall inception in transonic compressors. The casing groove is considered to have an influence to this flow interaction [8]; thus contributes in delaying the onset of stall. However, this literature focus only on the multiple grooves, which cause a difficulty in assessing the effect of each groove and to evaluate their contribution to the stability improvement.

In general, the near casing flow field in compressor is highly complicated due to various effects of secondary flow [9, 10]. This is especially prominent in the case when shock wave is involved with the passage flow field, such as in transonic compressors. The flow structure changes drastically along the blade chord, and therefore, the circumferential grooves applied at the endwall will interact with diverse flow field according to their locations [11]. This indicates the necessity to investigate the effect of casing treatment individually corresponding to its geometric parameters in order to understand the stall suppression mechanism of casing treatment in detail. But up to now, there still do not seem to be a detailed research on centrifugal compressor.

The objective of the present study is to obtain fundamental knowledge on the effect of the circumferentially grooved casing treatment on near-casing flow and stall margin of centrifugal compressor. First, numerical analysis of centrifugal compressor was conducted on smooth wall condition with detailed examination of the flow field characteristics at near stall condition. Next, parametric studies were carried out with respect to the radial location, the radial width, the axial depth of the single casing groove. Finally, numerical cases with different numbers of casing grooves were carried out to compare the results. The effect of casing groove to the compressor performance and near-tip flow structure was evaluated for each case based on stall margin improvement.

2. Analysis Model

As previously explained, a centrifugal compressor rotor was adopted in the present work. The specifications of the impeller and diffuser are summarized in Table 1. The overall performance and flow passage data obtained by experiment were referred for the validation of numerical modeling, which will be presented below.

Table 1. Geometric parameters of impeller and diffuser

Impeller		Diffuser	
Blade inlet diameter (mm)	140	The first vane inlet diameter (mm)	251.7
Blade outlet diameter (mm)	240	The first vane outlet diameter (mm)	296
Tip clearance (mm)	0.21	The second vane inlet diameter (mm)	300
Blade outlet width (mm)	12	The second vane outlet diameter (mm)	380
Number of rotor blades	9/9	Number of stator vanes	17
Rotation speed (rpm)	30215	Vane outlet width (mm)	12

3. Numerical Method

3.1. Numerical Scheme.

Steady flow simulations were performed by solving compressible Navier-Stokes equations. The three-dimensional Reynolds-averaged Navier-Stokes equations were discretized in the computational domain by a cell-centered finite volume method and advanced the solution in time using explicit fourth-order Runger-Kutta method. The one-equation Spalart-Allmaras turbulence model was adopted to evaluate the eddy viscosity. In order to guarantee convergence, the artificial viscosity coefficient is added. The local time step, implicit residual smoothing, multi-grid method are used to improve the convergence speed.

The total temperature and total pressure was applied for the inlet boundary condition. As for the outlet boundary condition, a given mass flow was imposed, different point corresponding to different mass flow rate, initial assumptions and give pressure value at the same time. Blade and wheel set as rotating parts, rotating speed as the design speed 30,215 RPM; Wheel cover part set as stationary part.

In calculation of this paper, through the increase or decrease gradually to a certain flow approximation numerical boundary point (nearly choke point and near surge point), the final solution convergence before the numerical instability is defined as a numerical boundary point (choke point and surge point).

3.2. Computational Grid.

The calculation was done for the whole centrifugal compressor. The H&I topology structure is used in grid generation of impeller, proper encryption in the blade leading edge and trailing edge, the number of nodes is 1,223,952. Two series of vane diffuser using the default topology of NUMECA, the grid number is 202,223 and 198,695 respectively. The grids of circumferential groove is generated by ZR Effect function in Autogrid5. The grids of circumferential groove and blade channel are connected by full no-matching boundary (FNMB). The grid node of circumferential groove casing treatment in three directions is 41, 37, 37, respectively, the total number of nodes is 56,129. With a circumferential groove in the computational grid is shown in figure 1.

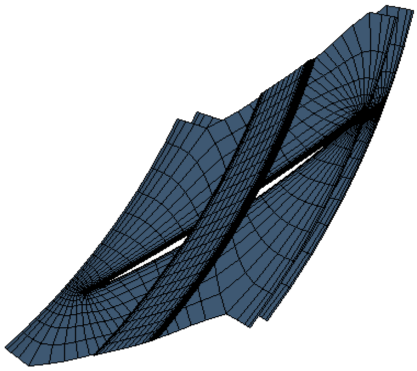

Figure 1. Computational grid with a circumferential groove

3.3. Validation.

The computational method was validated against the experimental datum. The overall characteristics are shown with the corresponding experimental data in figure 2. It can be seen from figure 2 that simulation gives a qualitatively good agreement with experimental results. In numerical simulations, the simple hypothesis for ideal gas, without considering the leakage loss, wheel resistance loss, constancy hypothesis do not tally with the actual situation and other factors, the efficiency and pressure ratio of the experiment are lower than the calculated result, but the overall trend is apparent, the computational method is able to predict the flow with sufficient reliability.

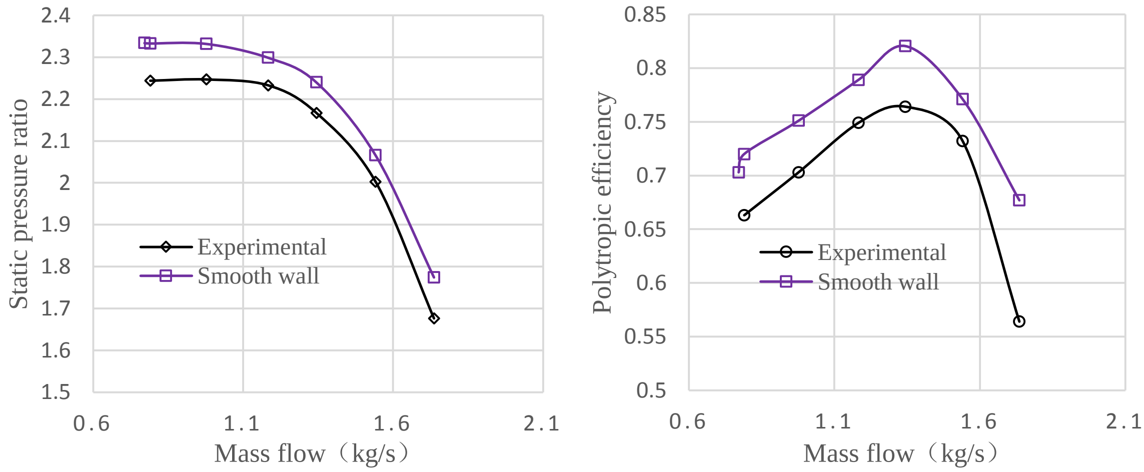

Figure 2. Characteristics plot of no-treated centrifugal compressor

4. Results and Discussion

4.1. Stall Characteristics and the Design of Circumferential Groove

4.1.1. Stall Characteristics in Diffuser. It is generally believed that the circumferential groove slot position depends on the magnitude of the location of the stall. Numerical simulation of the smooth wall found that in the near-stall condition, the deterioration of air flow in the impeller, lead to flow at a huge impact angle into diffuser leading edge, and made air separation and backflow on the no-working face of the first diffuser vanes. Figure 3 shows the Velocity streamlines at 95% span of diffuser in near-stall condition. Other than this, any notable vortex is not found among the passage. This implies that the flow which acts a dominant role in stall inception of the centrifugal compressor may range in the region near the casing.

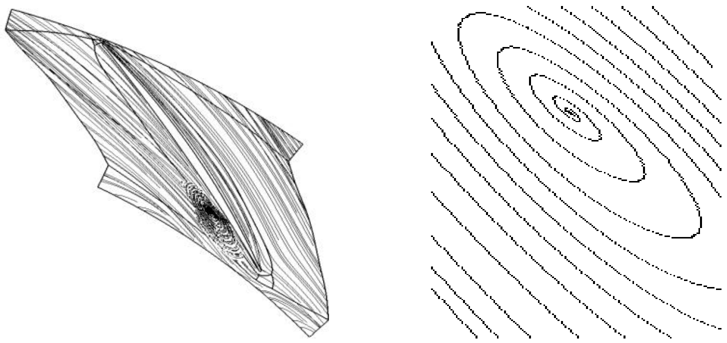

(a) Diffuser map (b) Partial enlargement of vortex

Figure 3. Velocity streamlines at 95% span of diffuser in near-stall condition

4.1.2. The design of Circumferential Groove. In this paper, the circumferential groove slot position designed in the first vane and the leading edge of the second vane of diffuser where stall occurred.

In order to determine the best slot position of the circumferential groove, a series of radial location of circumferential grooves were designed along the wheel side of the diffuser and numerical simulations were carried out. The circumferential groove with radial width of 6 mm and axial depth of 6 mm as initial. Figure 4 shows the slot location of circumferential grooves. For purpose of highlight the circumferential groove geometry characteristics, the circumferential groove naming rules would be designed as "axial depth _radial width_ the maximum absolute value of coordinates Y". Such as the number 2 circumferential groove in figure 4 is named as “6_6_139”.

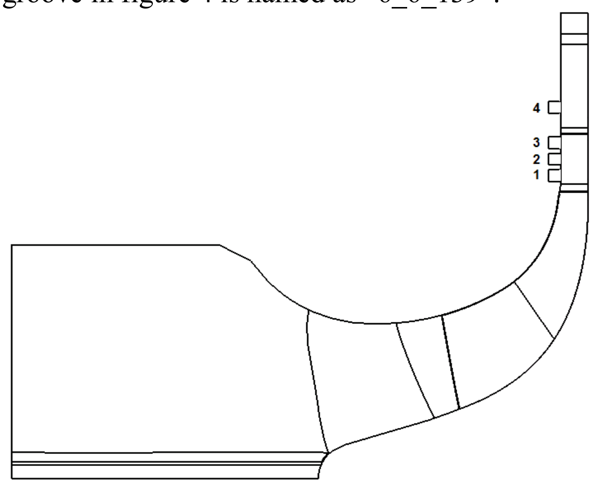

Figure 4. The slot location of circumferential grooves

For the sake of quantitative the improvement in stall margin and the influence of stage efficiency by circumferential groove, stable working range Φ, comprehensive improvement of stall margin $\Delta\Phi$, polytropic efficiency improvement at designed point $\Delta\eta_{pol}$ were evaluated in present work.

$$\Phi = \frac{Q_{m,des} - Q_{m,surge}}{Q_{m,des}} \times 100\%$$

$$\Delta\Phi = \frac{(Q_{m,surge})_{SW}}{(Q_{m,surge})_{CT}} \times \frac{(\varepsilon_{surge})_{CT}}{(\varepsilon_{surge})_{SW}} - 1 \tag{1}$$

$$\Delta\eta_{pol} = \frac{(\eta_{pol,des})_{CT}}{(\eta_{pol,des})_{SW}} - 1$$

4.2. Effect of Applying Circumferential Groove

4.2.1. Different radial location of circumferential grooves. Table 2 lists the specific calculation results of different radial location of circumferential grooves as “6_6_131”, “6_6_139”, “6_6_147” and “6_6_159". Figure 5 shows characteristics plot of different radial location of circumferential grooves.

Compared with the results of the smooth wall, it can be found from Table 2 and figure 5 that the circumferential groove number 1 (6_6_131) reached the largest stable working range of 47.48% and the most comprehensive stall margin improvement of 9.10%, but also caused the efficiency of the compressor design points reduced by 0.28%. In the circumferential groove number 2 (6_6_139) had smaller efficiency to reduce by 0.23%, and stable working range is 47.11%, 8.37% stall margin improvement. In addition, it can be found from Table 2 that the circumferential grooves located in the leading edge of the first vane of diffuser can get a better expanding stability than the other circumferential grooves, it can be explained by the stall location which near the leading edge in diffuser.

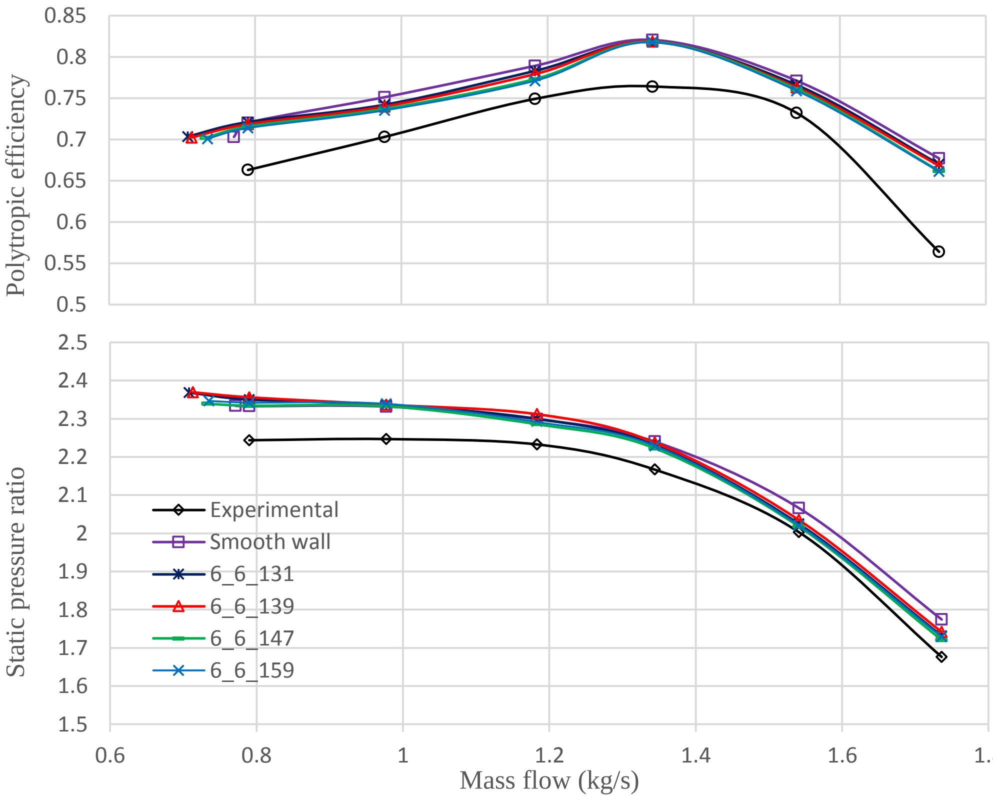

Figure 5. Characteristics plot of different radial location of circumferential grooves

Table 2. Results of different radial location of circumferential grooves

Circumferential groove	6_6_131	6_6_139	6_6_147	6_6_159	SW
Numbering scheme	1	2	3	4	-
$Q_{m,surge}$(kg/s)	0.708	0.713	0.733	0.735	0.771
ε_{surge}	2.3686	2.3694	2.3397	2.3465	2.3642
$\eta_{pol,des}$	0.8181	0.8185	0.8179	0.8177	0.8204
Φ	47.48%	47.11%	45.62%	45.47%	42.80%
$\Delta\Phi$	9.10%	8.37%	4.09%	4.11%	-
$\Delta\eta_{pol}$	-0.28%	-0.23%	-0.30%	-0.33%	-

4.2.2. Different radial width of circumferential grooves. Table 3 lists the specific calculation results of different radial width of circumferential grooves as “6_6_139”, “6_10_139” and “6_14_139”. Figure 6 shows characteristics plot of different radial width of circumferential grooves.

Compared with the results of the smooth wall, it can be found from Table 3 and figure 6 that the circumferential groove radial width increased from 6 mm to 10 mm, stable working range and comprehensive stall margin improvement enhanced with static pressure ratio fell and the efficiency decreases obviously; when the radial width increase from 10 mm to 14 mm, the static pressure continue to fall, stable working range and comprehensive stall margin improvement continue to increase, while the increasing amplitude is reduced, and the efficiency continue to decline.

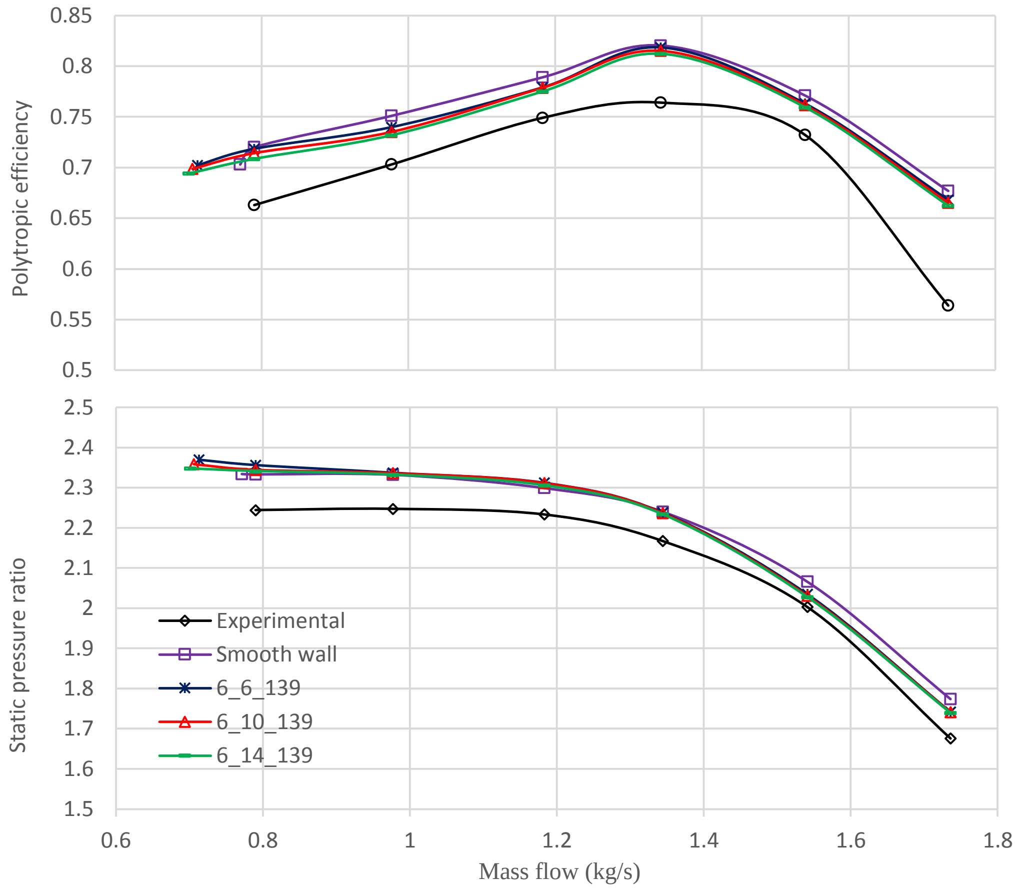

Figure 6. Characteristics plot of different radial width of circumferential grooves

Table 3. Results of different radial width of circumferential grooves

Circumferential groove	6_6_139	6_10_139	6_14_139	SW
$Q_{m,surge}$(kg/s)	0.713	0.706	0.701	0.771
ε_{surge}	2.3694	2.3583	2.3476	2.3642
$\eta_{pol,des}$	0.8185	0.8152	0.8123	0.8204
Φ	47.11%	47.63%	48.00%	42.80%
$\Delta\Phi$	8.37%	8.93%	9.21%	-
$\Delta\eta_{pol}$	-0.23%	-0.63%	-0.99%	-

4.2.3. Different axial depth of circumferential grooves. Table 4 lists the specific calculation results of different axial depth of circumferential grooves as “6_6_139”, “10_6_139” and “14_6_139”. Figure 7 shows characteristics plot of different axial depth of circumferential grooves.

Compared with the results of the smooth wall, it can be found from Table 4 and figure 7 that the circumferential groove axial depth increased from 6 mm to 10 mm, stable working range and comprehensive stall margin improvement enhanced with static pressure ratio fell and the efficiency decreases obviously; when the axial depth increase from 10 mm to 14 mm, stable working range and comprehensive stall margin improvement continue to increase, while the increasing amplitude is reduced, and the efficiency continue to decline.

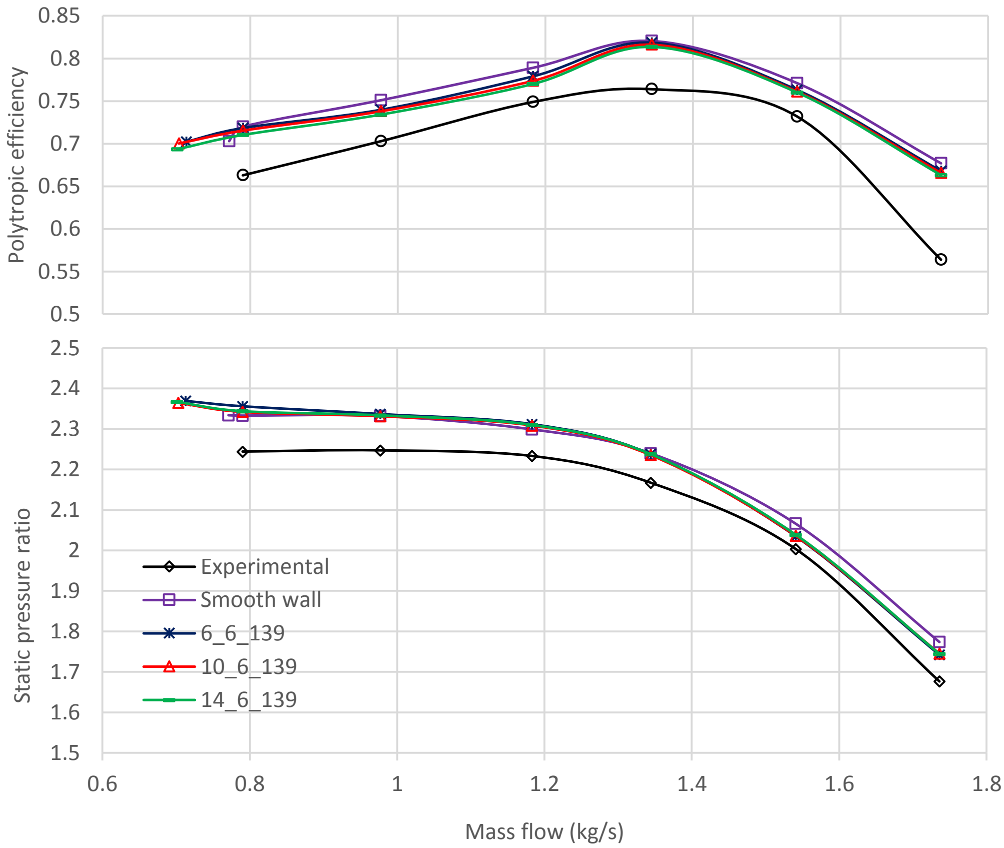

Figure 7. Characteristics plot of different axial depth of circumferential grooves

Table 4. Results of different axial depth of circumferential grooves

Circumferential groove	6_6_139	10_6_139	14_6_139	SW
$Q_{m,surge}$(kg/s)	0.713	0.703	0.701	0.771
ε_{surge}	2.3694	2.3647	2.3668	2.3642
$\eta_{pol,des}$	0.8185	0.8163	0.8136	0.8204
Φ	47.11%	47.85%	48.00%	42.80%
$\Delta\Phi$	8.37%	9.70%	10.11%	-
$\Delta\eta_{pol}$	-0.23%	-0.50%	-0.83%	-

4.2.4. Different numbers of circumferential grooves. Table 5 lists the specific calculation results of different numbers of circumferential grooves as "6_6_139_1" ("6_6_139"), "6_6_139_2" ("6_6_131" and "6_6_139") and "6_6_139_3" ("6_6_131", "6_6_139" and "6_6_147"). Figure 8 shows characteristics plot of different numbers of circumferential grooves.

Compared with the results of the smooth wall, it can be found from Table 5 and figure 8 that the circumferential groove number increased from 1 to 2, stable working range and comprehensive stall margin improvement enhanced with static pressure ratio fell and the efficiency decreases obviously; when the circumferential groove number increase from 2 to 3, stable working range and comprehensive stall margin improvement continue to increase, while the increasing amplitude is reduced, and the static pressure continue to decline, efficiency decreases more.

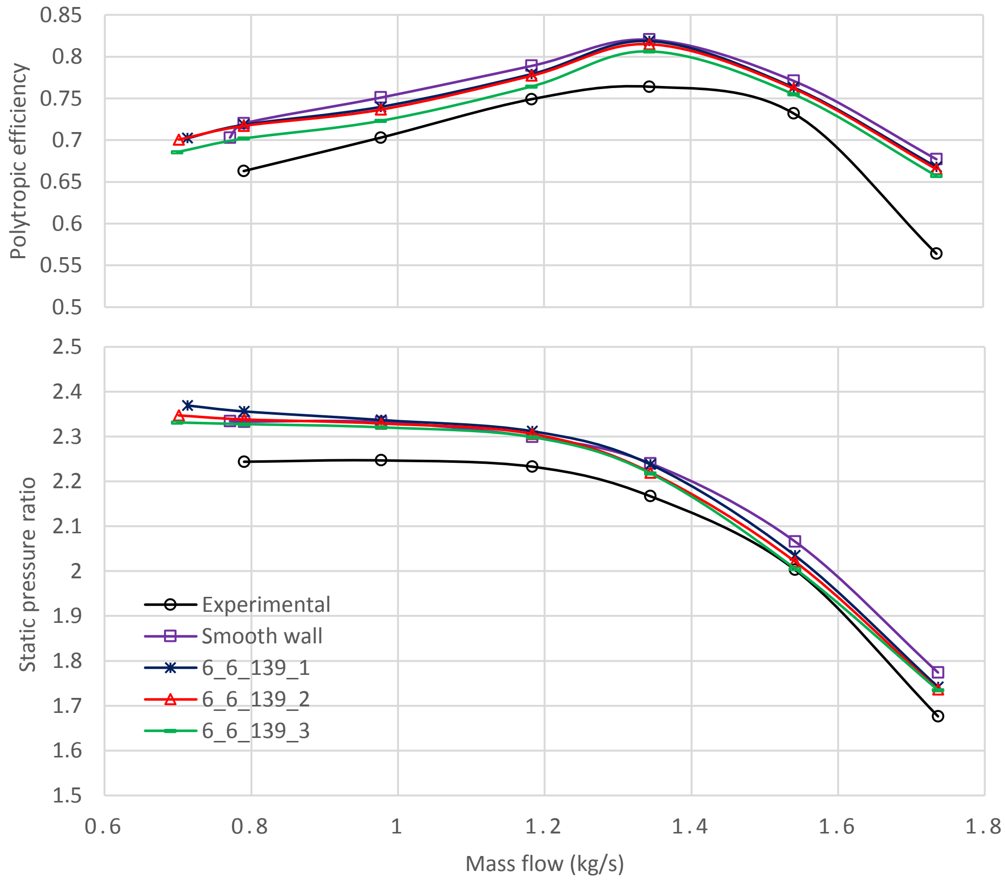

Figure 8. Characteristics plot of different numbers of circumferential grooves

Table 5. Results of different numbers of circumferential grooves

Circumferential groove	6_6_139_1	6_6_139_2	6_6_139_3	SW
$Q_{m,surge}$(kg/s)	0.713	0.701	0.699	0.771
ε_{surge}	2.3694	2.3468	2.3312	2.3642
$\eta_{pol,des}$	0.8185	0.8148	0.8063	0.8204
Φ	47.11%	48.00%	48.15%	42.80%
$\Delta\Phi$	8.37%	9.18%	8.76%	-
$\Delta\eta_{pol}$	-0.23%	-0.68%	-1.72%	-

5. Concluding Remarks

Steady three-dimensional Navier-Stokes flow simulations were conducted to investigate the effect of circumferential grooved casing treatment in vane diffuser of a centrifugal compressor. The conclusions are summarized as follows:

(1) In the centrifugal compressor, a tip leakage vortex was seen in near-stall condition. Numerical simulation of the smooth wall found that in the near-stall condition, the deterioration of air flow in the impeller, lead to flow at a huge impact angle into diffuser leading edge, and made flow separation and backflow on the suction face of the first diffuser vanes.

(2) When the groove is applied at the endwall of the diffuser, suitable position of circumferential groove can effectively expand the scope of the stable operation of the compressor, and efficiency has fallen a little at the design point.

(3) The width and depth of circumferential groove was increased, the stable working range and comprehensive stall margin improvements increase too, but the efficiency is decreased; the width and depth increasingly, stable working range and comprehensive stall margin improvements continue to increase, while the increasing amplitude is reduced, and efficiency is decreased more.

(4) The number of circumferential groove was increased, stable working range and comprehensive stall margin improvement enhanced with static pressure ratio fell and the efficiency decreases obviously; when the number of circumferential groove increasingly, stable working range and comprehensive stall margin improvement continue to increase, while the increasing amplitude is reduced, and the static pressure continue to decline, efficiency decreases more.

(5) The evaluation based on stall margin improvement showed the optimal position for the groove to be located was indicated to exist near the leading edge of the diffuser, and a combination of position, width, depth and numbers of circumferential grooves that will maximize both surge margin range and efficiency.

Nomenclature

Q = quantity of flow
ε = static pressure ratio
η = efficiency
Φ = stable working range
$\Delta\ \Phi$ = comprehensive improvement of stall margin
$\Delta\ \eta$ = efficiency improvement

Subscripts

m = mass
surge = surge point condition
pol = polytropic
des = design point

SW = smooth wall case
CT = casing treatment case

References

[1] Osborn W M, Lewis G W and Heidelberg L J 1971 Paper No. NASA TN D-6537
[2] Danner F C T, Kau H P, Muller M M, Schiffer H P and Brignole G A 2009 *ASME* Paper NO. GT2009-59647
[3] Lin F, Ning F and Liu H 2008 *ASME* Paper NO. GT2008-51541
[4] Houghton T and Day I 2009 *ASME* Paper NO. GT2009-59210
[5] Muller M W, Schiffer H P, Biela C and Hah C 2008 *ASME* Paper NO. GT2008-50135
[6] Chen H, Huang X, Shi K, Fu S, Bennington M A, Morris S C, Ross M, McNulty S and Wadia A 2010 *ASME* Paper NO. GT2010-23606
[7] Iyengar V and Lakshmi S 2005 *AIAA* 2005-0632
[8] Flisher F B 1989 *SAE transactions* **97** 1303-1310.
[9] Hunziker R, Dickmann H P, Emmrich R 2001 *Journal of Power and Energy* **215** 783-791.
[10] Xu W, Wang T and Gu CG 2011 *Science China Technological Sciences* **54(9)** 2483-2492.
[11] Zhu J and Chu W 2005 *AIAA* **809** 10-13.